NASA TECHNICAL NOTE

NASA TN D-4060

NASA TN D-4060

AN APPROXIMATE ANALYSIS OF THE EFFECTS OF NITROGEN INJECTION INTO THE BOUNDARY LAYER ON A GRAPHITE SURFACE IN A HIGH-TEMPERATURE DISSOCIATED AIRFLOW

by Kenneth C. Weston

Manned Spacecraft Center
Houston, Texas

NATIONAL AERONAUTICS AND SPACE ADMINISTRATION • WASHINGTON, D. C. • JULY 1967

AN APPROXIMATE ANALYSIS OF THE EFFECTS OF NITROGEN INJECTION INTO THE BOUNDARY LAYER ON A GRAPHITE SURFACE IN A HIGH-TEMPERATURE DISSOCIATED AIRFLOW

By Kenneth C. Weston

Manned Spacecraft Center
Houston, Texas

NATIONAL AERONAUTICS AND SPACE ADMINISTRATION

For sale by the Clearinghouse for Federal Scientific and Technical Information
Springfield, Virginia 22151 – CFSTI price $3.00

ABSTRACT

This study considers the effects of injection of a nonreacting gas (taken to be nitrogen) on the heat and mass transfer of a porous, chemically reacting surface (graphite) at hypersonic speeds. Heat and mass transfer relations are obtained for the carbon surface.

Numerical results are presented for the case of the sphere stagnation point at hypersonic speeds. Reductions in carbon surface mass loss and aerodynamic heating as a result of nitrogen injection are demonstrated. Comparisons with more rigorous digital computer solutions for zero nitrogen injection show the same qualitative trends and numerical differences of about 10 percent.

AN APPROXIMATE ANALYSIS OF THE EFFECTS OF NITROGEN INJECTION INTO THE BOUNDARY LAYER ON A GRAPHITE SURFACE IN A HIGH-TEMPERATURE DISSOCIATED AIRFLOW

By Kenneth C. Weston
Manned Spacecraft Center

SUMMARY

This study considers the effects of injection of a nonreacting gas (taken to be nitrogen) on the heat and mass transfer of a porous, chemically reacting surface (graphite) at hypersonic speeds. All chemical reactions are considered to occur in a reacting sheet adjacent to the wall. Equations for the determination of species mass fractions at the wall are derived under the assumptions of a frozen boundary layer and chemical equilibrium in the flame sheet. Schmidt and Prandtl numbers are taken as unity. Heat and mass transfer relations are obtained for the carbon surface.

Numerical results are presented for the case of the sphere stagnation point at hypersonic speeds. Reductions in carbon surface mass loss and aerodynamic heating as a result of nitrogen injection are demonstrated. Comparisons with more rigorous digital computer solutions for zero nitrogen injection show the same qualitative trends and numerical differences of about 10 percent.

INTRODUCTION

Graphite is considered frequently as a heat-protection material for the leading edges and other high heating-rate areas of lifting reentry vehicles. Its ability to sustain high temperatures and its strength at elevated temperatures make it particularly suitable for such applications. These unusual qualities have motivated considerable analytical study of the ablative behavior of graphite. Moreover, its elemental nature offers substantial analytical simplifications relative to chemically complex organic ablators. The present work utilizes this simplicity to examine the effects on heat and mass transfer of injection of nonreacting nitrogen through porous graphite.

A number of investigators have analyzed the behavior of the flow over an ablating substance within the framework of boundary-layer theory. In 1957, Dennison and Dooley (ref. 1) treated the laminar boundary layer with combustion using a model very much like that employed in the present study. This model assumes all chemical reactions to occur at a surface to which oxygen and fuel are transported by convection and diffusion. Chemical equilibrium is assumed to exist at this surface; combustion

products diffuse in both directions from the surface. As a further simplification, reference 1 utilized constant property boundary-layer solutions for Lewis and Prandtl numbers of unity.

In 1962 and 1964, S. Scala (refs. 2 and 3) presented the results of sophisticated calculations of the ablation of graphite. These digital computer solutions of the reacting gas boundary layer included consideration of nine chemical components and six chemical reactions in the boundary layer. The calculations involved simultaneous integration of coupled boundary-layer equations including calculations of transport properties based on multicomponent diffusion rather than the frequently employed binary model. These calculations show distributed reaction zones within the boundary layer, and are the most detailed results presently available for graphite ablation.

In reference 4, Lees concluded that, for a Lewis number of unity, reaction rates in the boundary layer play a secondary role in determining the mass fractions of chemical species at the surface and transport properties. His analysis also suggests that combustion may be beneficial in reducing heat transfer if the heat of sublimation is comparable to the heat reaction. Lees further stated that these conclusions are independent of the model of chemical reaction assumed.

Dorrance outlined a method in reference 5 for the analysis of the reacting laminar boundary layer on a carbon surface. His analysis considered all reactions to occur at the wall, with the boundary layer treated as nonreacting. The present work extends this analysis, for the case of Prandtl and Schmidt numbers of unity, to the case of nitrogen injected into a porous carbon surface.

This work is based on research documented in a Master's Thesis at Rice University in 1965. Discussions with Dr. Frederic A. Wierum of Rice University are gratefully acknowledged.

SYMBOLS

B	mass transfer parameter
C	species mass fractions
$\bar{C}$	elemental mass fractions
C_H	Stanton number
c_p	specific heat at constant pressure
D	diffusion coefficient
f	modified stream function (see equations (59), (60), and (61))
G	function defined by equation (74)

g	dimensionless enthalpy, $\frac{I}{I_e}$
(g)	gaseous phase
h	local static enthalpy
h_{eff}	effective heat of ablation
h_i	enthalpy of the i'th specie
h_i^o	heat of reaction of the i'th specie
I	stagnation enthalpy
J_1, J_2, J_3	quantities defined in equations (38) to (40)
K_1, K_2, K_3, K_4	equilibrium constants defined in equations (1) to (4)
k	thermal conductivity
L	Lewis number, $\frac{\rho D c_p}{k}$
L_{vc}	heat of sublimation of graphite
ℓ	density-viscosity ratio defined in equation (63)
M	molecular weight
$\overline{M}$	mean molecular weight defined in equation (81)
M^*	Mach number
M_a	molecular weight of undissociated air
M_e^*	Mach number at edge of boundary layer
$\dot{m}_C$	mass flux of carbon
$\dot{m}_E$	total mass flux from equilibrium layer defined in equation (10)
$\dot{m}_N$	mass flux of nitrogen

P	Prandtl number, $\frac{\mu c_p}{k}$
p	pressure
$\dot{q}$	heat flux
$\dot{q}_h$	energy absorbed in steady ablation
$\dot{q}_{rad}$	radiative heat flux from surface
$\dot{q}_s$	heat flux to graphite surface
$\dot{q}_w$	aerodynamic heat flux with mass injection effects included
R	sphere radius of curvature
$\mathcal{R}$	universal gas constant
R_i	gas constant for i'th specie
r	radius normal to body axis of symmetry extending to body surface
S	Schmidt number, $\mu/\rho D$
s	coordinate along body surface
(s)	solid phase
$\bar{s}$	boundary-layer coordinate defined by equation (58)
T	temperature
T^+	reference temperature defined by equation (79)
t	time
u	local velocity parallel to wall
v	local velocity normal to wall
$\dot{w}_i$	rate of production of the i'th specie
X	$\left[\sum_i p_i M_i\right]^{-1}$, equation (30)

x_i	mole fraction of the i'th specie
y	coordinate normal to wall
Z_i	dimensionless mass fraction of i'th specie, $\frac{C_i}{C_{i,e}}$
δ	thickness of equilibrium layer
η	boundary-layer coordinate defined in equation (57)
η^*, η^{**}	dummy variables
λ	generalizing variable representing f', g, or Z_i
μ	viscosity coefficient
ν	index, $\nu = 0$ for planar flow, $\nu = 1$ for axisymmetric flow
ρ	density
τ	thickness of graphite layer
ϕ	generalizing variable representing 1, P, or S
ψ	stream function

Subscripts:

A	air
E	condition in equilibrium layer
e	condition at outer edge of boundary layer
f	frozen
i	of i'th specie
in	initial
M	arithmetic mean value
N. B.	no mass injection
sp	stagnation point

w	conditions at wall
∞	ahead of bow shock

ANALYSIS

Analytical Model

The ablation of graphite at hypersonic speeds occurs through sublimation and chemical reactions with the surrounding air. At wall temperatures below about 1000° K the rate of mass loss is governed by the rate of oxidation of the graphite surface. At slightly higher temperatures a transition region precedes a third region in which the rate of surface recession is governed by the rate of diffusion of oxygen into the boundary layer. This "diffusion-controlled regime" prevails over a range of wall temperatures from about 1500° to about 3000° K at atmospheric pressure. The present analysis considers the effects of nitrogen injection on graphite ablation in this regime. At temperatures above 3000° K the rate of sublimation of carbon exceeds the rate of diffusion of oxygen, and uncombined gaseous carbon molecules exist at the wall in significant amounts. In this regime nitrogen reactions with graphite yield sizable mass fractions of cyanogen.

The present study considers the ablation of graphite for the diffusion-controlled regime in terms of a model in which the rate of diffusion of oxygen to the chemically active graphite surface is governed by mathematical solutions for a frozen boundary layer. The boundary layer is frequently termed frozen when the rate of generation of species in it is negligible. Such solutions have been successful in predicting heat transfer in dissociated-air boundary layers in which the wall catalyzes atom recombination and the wall temperatures are well below the boundary-layer-edge temperature (refs. 4 to 6). It is therefore assumed that all chemical reactions occur in an infinitesimal layer adjacent to the wall in which chemical equilibrium exists. This "equilibrium layer" is a region where nitrogen and carbon are received from the ablating surface, chemical reactions occur with oxygen from the boundary layer, and the equilibrium mixture is supplied to the boundary layer. In view of the approximation imposed by some of the necessary assumptions, it is reasonable to take advantage of the great simplifications made possible by assuming Prandtl, Schmidt, and, therefore, Lewis numbers to be unity. These assumptions are perhaps best justified by the remarkable agreement of the present calculations with the results of reference 3 which were obtained with state-of-the-art transport properties.

The present analysis is limited to hypersonic conditions for which the species at the edge of the boundary layer are atomic or molecular. Moreover, the boundary-layer-edge composition is assumed to be made up of nitrogen and oxygen only. Boundary-layer-edge conditions are obtained from the normal shock conservation equations, the assumption of isentropic and isoenthalpic flow along the body streamline, and the real air properties of reference 7. Absence of consideration of ions and electrons at the boundary-layer edge limits the applicability of this analysis to boundary-layer-edge temperatures below 10 000° K. This is well beyond the maximum equilibrium-shock-layer temperatures encountered, for example, during the reentry of current manned orbital vehicles.

The thermal decomposition of a graphite surface has been studied by many investigators. While carbon molecules (atomic carbon C and higher mass carbon radicals such as $C_2, C_3, C_4, \ldots, C_n$) may sublime from a hot carbon surface, experimental evidence indicates that C_3 and C are most abundant over a wide range of temperatures (refs. 3 and 8). In the present analysis it is assumed that the sole product of carbon mass loss is gaseous C_3. Dissociation of C_3 to C and subsequent reactions with oxygen to produce carbon monoxide are allowed in the equilibrium layer. Formation of carbon dioxide is not considered since it has been shown in reference 3 to be present only as a trace specie in the temperature range of interest. The analysis is therefore based on the assumed heterogeneous surface reaction

$$C_3(s) \rightleftharpoons C_3(g)$$

and the following homogeneous reactions in the equilibrium layer

$$C_3(g) \rightleftharpoons 3C(g)$$

$$2C(g) + O_2(g) \rightleftharpoons 2CO(g)$$

$$C(g) + O(g) \rightleftharpoons CO(g)$$

where (s) and (g) indicate solid and gaseous phases, respectively.

The results of reference 3 show that nitrogen reactions are insignificant in the temperature range-of-interest. In this case nitrogen acts only as a diluent. Moreover, nitrogen is present in the equilibrium layer in diatomic form only; the range of wall temperatures considered is too low for significant dissociation.

Composition of the Equilibrium Layer

The partial pressures of the species in the four chemical reactions listed may be related through the following expressions for the equilibrium constants:

$$K_1(T) = p_{C_3} \tag{1}$$

$$K_2(T) = p_C^3 \Big/ p_{C_3} \tag{2}$$

$$K_3(T) = p_{CO}^2 / p_{O_2} p_C^2 \tag{3}$$

$$K_4(T) = p_{CO} / p_C p_O \tag{4}$$

The partial pressure of C_3 is given by Thorne and Winslow (ref. 8) in the vicinity of 2400° K as

$$\log p_{C_3} = 9.811 - \frac{40\,296}{T} \tag{5}$$

where T and p are specified in °K and atmospheres. Thus the partial pressure of C_3 at the wall is determined when the wall temperature is specified. The partial pressures of the other species, except diatomic nitrogen N_2, may be expressed in terms of the partial pressure of carbon monoxide and the equilibrium constants as follows:

$$p_C = K_1^{1/3} K_2^{1/3} \tag{6}$$

$$p_{O_2} = \left(K_3^{-1} K_1^{-2/3} K_2^{-2/3}\right) p_{CO}^2 \tag{7}$$

$$p_O = \left(K_4^{-1} K_1^{-1/3} K_2^{-1/3}\right) p_{CO} \tag{8}$$

The pressure at the wall is related to the partial pressures of the above species and nitrogen by Dalton's law of partial pressure

$$p_{N_2} + p_{O_2} + p_O + p_C + p_{C_3} + p_{CO} = p_E = p_e = p_w \tag{9}$$

The latter equality follows from the usual assumption of constancy of pressure across a boundary layer. To obtain the expression for the partial pressure of carbon monoxide necessary to determine partial pressures of the other species in the equilibrium layer, the convection and diffusion of species and mass injection at the wall must be considered.

Mass Balance

Consider the flux of mass through the equilibrium layer at the wall as shown in the following sketch. In general, nitrogen and carbon are uniformly injected into the

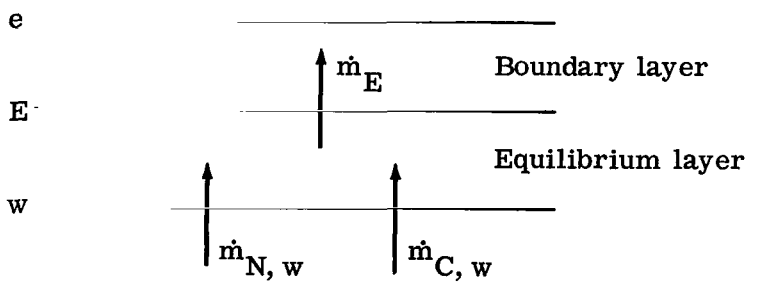

equilibrium layer and a net mass flux $\dot{m}_E$ from the equilibrium layer into the boundary layer is defined. Then for steady flow

$$\dot{m}_E = \dot{m}_{N,w} + \dot{m}_{C,w} \tag{10}$$

Expressions may also be written for the accumulation of mass of each of the elements C, N, and monatomic oxygen O in the infinitesimal equilibrium layer. For a steady flow of each of the elemental mass fractions, the net rate of storage of each element must be zero. The following relations must then be satisfied:

$$\delta\rho \frac{d\bar{C}_C}{dt} = \dot{m}_{C,w} - \dot{m}_E \bar{C}_{C,E} + \left(\rho D \frac{\partial \bar{C}_C}{\partial y}\right)_E = 0 \tag{11}$$

$$\delta\rho \frac{d\bar{C}_N}{dt} = \dot{m}_{N,w} - \dot{m}_E \bar{C}_{N,E} + \left(\rho D \frac{\partial \bar{C}_N}{\partial y}\right)_E = 0 \tag{12}$$

$$\delta\rho \frac{d\bar{C}_O}{dt} = -\dot{m}_E \bar{C}_{O,E} + \left(\rho D \frac{\partial \bar{C}_O}{\partial y}\right)_E = 0 \tag{13}$$

For later reference, equations (11) to (13) may be written

$$\dot{m}_{C,\,w} + \dot{m}_{N,\,w} = \dot{m}_{N,\,w} + \dot{m}_E \overline{C}_{C,\,E} - \left(\rho D \frac{\partial \overline{C}_C}{\partial y}\right)_E \tag{14}$$

$$\dot{m}_{N,\,w} = \dot{m}_E \overline{C}_{N,\,E} - \left(\rho D \frac{\partial \overline{C}_N}{\partial y}\right)_E \tag{15}$$

$$0 = m_E \overline{C}_{O,\,E} - \left(\rho D \frac{\partial \overline{C}_O}{\partial y}\right)_E \tag{16}$$

It is shown subsequently that when the Prandtl, Schmidt, and Lewis numbers are unity, the velocity, enthalpy, and elemental mass fraction profiles are linearly related. Therefore,

$$\overline{C} = \overline{C}_E + \frac{\overline{C}_e - \overline{C}_E}{I_e - I_E}\left(I - I_E\right) \tag{17}$$

where

$$I = \sum_i C_i \left(\int_0^T c_{p,\,i}\, dT\right) + \sum_i C_i h_i^{\,o} + u^2/2$$

Then

$$\frac{\partial \overline{C}}{\partial y} = \frac{\overline{C}_e - \overline{C}_E}{I_e - I_E}\,\frac{\partial I}{\partial y}$$

and the diffusion term in equations (14) to (16) may be expressed in terms of the Stanton number

$$\left(\rho D \frac{\partial \overline{C}}{\partial y}\right)_E = \left(\overline{C}_e - \overline{C}_E\right)\left(\frac{L \frac{k}{c_p}\,\frac{\partial I}{\partial y}}{I_e - I_E}\right)_E = \left(\overline{C}_e - \overline{C}_E\right)\rho_e u_e C_H \tag{18}$$

where $L = 1$ and the Stanton number C_H is given by

$$\rho_e u_e C_H = \frac{\left(\frac{k}{c_p}\frac{\partial I}{\partial y}\right)_E}{I_e - I_E}$$

The diffusion terms in equations (14) to (16) may be eliminated by using equation (18). The resulting expressions are

$$\dot{m}_E = \dot{m}_{N,w} + \dot{m}_E \overline{C}_{C,E} - \left(\overline{C}_{C,e} - \overline{C}_{C,E}\right) \rho_e u_e C_H \tag{19}$$

$$\dot{m}_{N,w} = \dot{m}_E \overline{C}_{N,E} - \left(\overline{C}_{N,e} - \overline{C}_{N,E}\right) \rho_e u_e C_H \tag{20}$$

$$0 = \dot{m}_E \overline{C}_{O,E} - \left(\overline{C}_{O,e} - \overline{C}_{O,E}\right) \rho_e u_e C_H \tag{21}$$

where equation (10) has been used to eliminate the injection rate of carbon at the wall.

A mass injection parameter B is defined as

$$B = \frac{\dot{m}_E}{\rho_e u_e C_H} \tag{22}$$

Equations (19) to (21) become

$$(B + 1)\,\overline{C}_{C,E} = \overline{C}_{C,e} + B - \frac{\dot{m}_{N,w}}{\rho_e u_e C_H} \tag{23}$$

$$(B + 1)\,\overline{C}_{N,E} = \overline{C}_{N,e} + \frac{\dot{m}_{N,w}}{\rho_e u_e C_H} \tag{24}$$

$$(B + 1)\,\overline{C}_{O,E} = \overline{C}_{O,e} \tag{25}$$

Throughout the following pages the subscript w is omitted from the wall nitrogen-injection parameter $\frac{\dot{m}_{N,w}}{\rho_e u_e C_H}$ with the understanding that nitrogen injection through the wall is indicated.

Equations (23) to (25) represent the mass balances on the equilibrium layer in terms of the elemental mass fractions. These expressions may be rewritten in terms of species mass fractions. In so doing, the mass fractions of carbon at the edge of the boundary layer and the mass fraction of monatomic nitrogen at the wall are set equal to zero.

$$(B+1)\left[C_{C_3,E} + C_{C,E}\left(\frac{M_C}{M_{CO}}\right) C_{CO,E}\right] = B - \frac{\dot{m}_N}{\rho_e u_e C_H} \tag{26}$$

$$(B+1)\left(C_{N_2,E}\right) = \left(C_{N_2,e} + C_{N,e}\right) + \frac{\dot{m}_N}{\rho_e u_e C_H} \tag{27}$$

$$(B+1)\left(C_{O,E} + C_{O_2,E} + \frac{M_O}{M_{CO}} C_{CO,E}\right) = \left(C_{O,e} + C_{O_2,e}\right) \tag{28}$$

It is desirable to write the mass fractions in the equilibrium layer in terms of partial pressures of the species. The partial pressure and the mass fraction of the i'th specie are related by

$$C_i = p_i M_i X \tag{29}$$

where

$$X = \frac{1}{\sum_i p_i M_i} \tag{30}$$

Equations (26) to (28) become

$$(B + 1)\left(M_{C_3} p_{C_3, E} + M_C P_{C, E} + M_C p_{CO, E}\right) X_E = B - \frac{\dot{m}_N}{\rho_e u_e C_H} \tag{31}$$

$$(B + 1)\left(M_{N_2} p_{N_2, E}\right) X_E = C_{N_2, e} + C_{N, e} + \frac{\dot{m}_N}{\rho_e u_e C_H} \tag{32}$$

$$(B + 1)\left(M_O p_{O, E} + M_{O_2} p_{O_2, E} + M_O p_{CO, E}\right) X_E = C_{O, e} + C_{O_2, e} \tag{33}$$

All of the basic relations are now available to solve for the partial pressures of the species in the equilibrium layer. From equation (32) the partial pressure of diatomic nitrogen N_2 is given by

$$p_{N_2, E} = \frac{C_{N_2, e} + C_{N, e} + \dfrac{\dot{m}_N}{\rho_e u_e C_H}}{(B + 1) X_E M_{N_2}} \tag{34}$$

Equation (33) may be used to eliminate $(B + 1) X_E$ from equation (34) yielding

$$p_{N_2, E} = \frac{\left(C_{N_2, e} + C_{N, e} + \dfrac{\dot{m}_N}{\rho_e u_e C_H}\right)\left(M_O p_{O, E} + M_{O_2} p_{O_2, E} + M_O p_{CO, E}\right)}{M_{N_2}\left(C_{O, e} + C_{O_2, e}\right)} \tag{35}$$

Using equations (7) and (8) the partial pressure of nitrogen may be expressed in terms of the partial pressure of carbon monoxide

$$p_{N_2,\,E} = \frac{\left(C_{N_2,\,e} + C_{N,\,e} + \frac{\dot{m}_N}{\rho_e u_e C_H}\right)\left(M_O K_4^{-1} K_1^{-1/3} K_2^{-1/3} p_{CO,\,E}\right)}{M_{N_2}\left(C_{O,\,e} + C_{O_2,\,e}\right)}$$

$$+ \frac{\left(C_{N_2,\,e} + C_{N,\,e} + \frac{\dot{m}_N}{\rho_e u_e C_H}\right)\left(M_{O_2} K_3^{-1} K_1^{-2/3} K_2^{-2/3} p_{CO,\,E}^{\,2} + M_O p_{CO,\,E}\right)}{M_{N_2}\left(C_{O,\,e} + C_{O_2,\,e}\right)} \tag{36}$$

Combining equation (36) with equations (1) and (6) to (9) yields a quadratic equation for $p_{CO,\,E}$

$$\frac{\left(C_{N_2,\,e} + C_{N,\,e} + \frac{\dot{m}_N}{\rho_e u_e C_H}\right)}{M_{N_2}\left(C_{O,\,e} + C_{O_2,\,e}\right)} \left[M_O\left(1 + K_4^{-1} K_1^{-1/3} K_2^{-1/3}\right) p_{CO,\,E}\right.$$

$$\left. + M_{O_2} K_3^{-1} K_1^{-2/3} K_2^{-2/3} p_{CO,\,E}^{\,2}\right] + \left(K_3^{-1} K_1^{-2/3} K_2^{-2/3}\right) p_{CO,\,E}^{\,2}$$

$$+ \left(K_4^{-1} K_1^{-1/3} K_2^{-1/3}\right) p_{CO,\,E} + K_1^{1/3} K_2^{1/3} + K_1 + p_{CO,\,E} - p_e = 0 \tag{37}$$

Let

$$J_1 = \frac{C_{N_2,\,e} + C_{N,\,e} + \frac{\dot{m}_N}{\rho_e u_e C_H}}{M_{N_2}\left(C_{O,\,e} + C_{O_2,\,e}\right)} \tag{38}$$

$$J_2 = 1 + K_4^{-1} K_1^{-1/3} K_2^{-1/3} \tag{39}$$

$$J_3 = K_3^{-1} K_1^{-2/3} K_2^{-2/3} \tag{40}$$

Expressed in terms of the J, equation (37) becomes

$$p_{CO,E}^2 + \frac{J_1 J_2 M_O + J_2}{J_1 J_3 M_{O_2} + J_3} p_{CO,E} + \frac{K_1^{1/3} K_2^{1/3} + K_1 - p_e}{J_1 J_3 M_{O_2} + J_3} = 0 \tag{41}$$

The complete solution for the partial pressure of carbon monoxide may be shown as

$$p_{CO,E} = 1/2 \left[\sqrt{\left(\frac{J_1 J_2 M_O + J_2}{J_1 J_3 M_{O_2} + J_3} \right)^2 + 4 \left(\frac{p_e - K_1 - K_1^{1/3} K_2^{1/3}}{J_1 J_3 M_{O_2} + J_3} \right)} - \frac{J_1 J_2 M_O + J_2}{J_1 J_3 M_{O_2} + J_3} \right] \tag{42}$$

Over a wide range of wall temperature and pressure, the squared term in the radical of equation (42) is large compared with the other term. Thus numerical difficulties are encountered in attempting to evaluate $p_{CO,E}$ using equation (42). Examination of the orders of magnitudes of the terms in equation (41) reveals that while $p_{CO,E}^2$ is of order one, the other two terms are many orders of magnitude larger. In this case $p_{CO,E}$ can be accurately calculated by neglecting $p_{CO,E}^2$ in equation (41). The following simpler expression is obtained

$$p_{CO,E} = \frac{p_e - K_1 - K_1^{1/3} K_2^{1/3}}{J_1 J_2 M_O + J_2} \tag{43}$$

This expression may be accurately employed for the determination of $p_{CO,E}$ when

$$\frac{J_1 J_2 M_O + J_2}{J_1 J_3 M_{O_2} + J_3} >> p_{CO,E} \tag{44}$$

Using equation (43) the partial pressures of the species other than CO may be expressed in terms of J as

$$p_{O_2,\,E} = J_3\left(\frac{p_e - K_1 - K_1^{1/3}K_2^{1/3}}{J_1J_2M_O + J_2}\right)^2 \tag{45}$$

$$p_{O,\,E} = (J_2 - 1)\left(\frac{p_e - K_1 - K_1^{1/3}K_2^{1/3}}{J_1J_2M_O + J_2}\right) \tag{46}$$

$$p_{C,\,E} = K_1^{1/3}K_2^{1/3} \tag{47}$$

$$p_{C_3,\,E} = K_1 \tag{48}$$

$$p_{N_2,\,E} = J_1\left(M_OJ_2p_{CO,\,E} + M_{O_2}J_3p_{CO,\,E}^2\right)$$

$$= p_e - p_{CO,\,E} - p_{O_2,\,E} - p_{O,\,E} - p_{C,\,E} - p_{C_3,\,E} \tag{49}$$

When the wall temperature, nitrogen injection parameter, and boundary-layer-edge conditions are specified, J can be calculated from equations (38) to (40); the equilibrium-layer partial pressures can be evaluated from equations (43) and (45) to (49), and B is determined from equation (32). To evaluate the heat and mass fluxes at the graphite surface the theory of the boundary layer must be considered.

Boundary Layer

The present analysis of the boundary layer follows the treatment of Dorrance in reference 5. The basic equations for the reacting gas boundary layer are presented.

Continuity:

$$\frac{\partial}{\partial s}\left(\rho u r^{\nu}\right) + \frac{\partial}{\partial y}\left(\rho v r^{\nu}\right) = 0 \tag{50}$$

S-momentum:

$$\rho u \frac{\partial u}{\partial s} + \rho v \frac{\partial u}{\partial y} = - \frac{dp}{ds} + \frac{\partial}{\partial y}\left(\mu \frac{\partial u}{\partial y}\right) \tag{51}$$

Y-momentum:

$$p = p_e = p_E \tag{52}$$

Energy:

$$\rho u \frac{\partial I}{\partial s} + \rho v \frac{\partial I}{\partial y} = \frac{\partial}{\partial y}\left[\frac{\mu}{P} \frac{\partial I}{\partial y} + \mu\left(1 - \frac{1}{P}\right) \frac{1}{2} \frac{\partial u^2}{dy}\right] - \frac{\partial}{\partial y}\left[\left(\frac{1}{L} - 1\right)\rho D \sum_i h_i \frac{\partial C_i}{\partial y}\right] \tag{53}$$

Species:

$$\rho u \frac{\partial C_i}{\partial s} + \rho v \frac{\partial C_i}{\partial y} = \frac{\partial}{\partial y}\left(\rho D \frac{\partial C_i}{\partial y}\right) + \dot{w}_i \tag{54}$$

State:

$$p_i = \rho_i R_i T \tag{55}$$

Enthalpy:

$$I = \sum_i C_i \left(\int_0^T c_{p,\,i}\, dT + h_i^{\,o}\right) + u^2/2 = h + u^2/2 \tag{56}$$

Equations (50) to (56) apply to the flow of a laminar boundary layer over a plane ($\nu = 0$) or axisymmetric ($\nu = 1$) surface. The gas is assumed to be an ideal gas and the diffusion process is assumed to be represented by binary diffusion according to Fick's law. Equations (50) to (56) are a set of nonlinear partial differential equations which are not generally solvable. A very useful technique for the solution of such equations is to transform the equations into ordinary differential equations. Solutions of this type are termed similar solutions. The transformation of equations (50) to (56) is derived in detail in reference 5. The equations are transformed into an $\eta, \bar{s}$ coordinate system in which

$$\eta = \frac{\rho_e u_e r^\nu}{(2\bar{s})^{1/2}} \int_0^y \frac{\rho}{\rho_e}\, dy \tag{57}$$

and

$$\bar{s} = \int_0^s \rho_e \mu_e r^{2\nu} u_e\, ds \tag{58}$$

A stream function which is the product of separate functions of η and s is introduced

$$\psi(s, \eta) = N(s)\, f(\eta) \tag{59}$$

The function $f(\eta)$ is defined such that

$$u = u_e f'(\eta) \tag{60}$$

The modified stream function at the wall f(0) is also related to the mass flow through the wall as

$$f(0) = \frac{-(\rho v)_E\, (2\bar{s})^{1/2}}{\rho_e u_e \mu_e r^\nu} \tag{61}$$

The dependent variable in the momentum equation becomes f, and ψ is eliminated. The resulting equation is then considered to be a function of η only. The resulting momentum equation becomes

$$(\ell f'')' + ff'' + \frac{2\bar{s}}{u_e}\frac{du_e}{d\bar{s}}\left(\frac{\rho_e}{\rho} - (f')^2\right) = 0 \tag{62}$$

where primes denote differentiation with respect to η and

$$\ell = \frac{\rho\mu}{\rho_e\mu_e} \tag{63}$$

It should be noted that similar solutions may be obtained for equation (62) only if the third term is a constant or a function of η only. This is the case for a stagnation point where

$$\frac{2\bar{s}}{u_e}\frac{du_e}{d\bar{s}} = \text{a constant}$$

or for a flat plate where

$$\frac{du_e}{d\bar{s}} = 0$$

If dimensionless enthalpy and species functions are defined as

$$g(\eta) = \frac{I}{I_e} \tag{64}$$

$$Z_i(\eta) = \frac{C_i}{C_{i,e}} \tag{65}$$

transformations of the energy and species equations may be written

$$\left(\frac{\ell}{\bar{P}}\,g'\right)' + fg' = \frac{2\bar{s}f'g}{I_e}\,\frac{dI_e}{d\bar{s}} + \left[\frac{\ell}{\bar{s}}\left(\frac{1}{L}-1\right)\sum_i \frac{h_i C_{i,e}}{I_e}\,Z_i'\right]' + \frac{u_e^2}{I_e}\left[\left(\frac{1}{\bar{P}}-1\right)\ell f'f''\right]' \tag{66}$$

and

$$\left(\frac{\ell}{\bar{s}}\,Z_i'\right)' + fZ_i' = \frac{2\bar{s}f'Z_i}{C_{i,e}}\,\frac{dC_{i_e}}{d\bar{s}} - \frac{2\bar{s}\dot{w}_i}{\rho\rho_e u_e^2 \mu_e r^{2\nu} C_{i,e}} \tag{67}$$

The boundary conditions on these equations are

$$f(0) = f_E = \frac{-(\rho v)_E (2\bar{s})^{1/2}}{\rho_e u_e \mu_e r^{\nu}}$$

$$f'(0) = 0 \qquad\qquad f'(\infty) = 1$$

$$Z_i(0) = Z_{i_E} = \frac{C_{i,E}}{C_{i,e}} \qquad\qquad Z_i(\infty) = 1$$

$$g(0) = g_E \qquad\qquad g(\infty) = 1$$

At this point it is desirable to attempt to simplify equations (62), (66), and (67). Lees (ref. 9) has pointed out that, in the presence of extreme cooling, the third term in equation (62) has only a weak effect on solutions of the stagnation-point problem. Therefore, it is assumed that this term is negligible compared with the first and second terms. On a flat plate with no pressure gradient $\frac{du_e}{d\bar{s}} = 0$ and the third term is identically zero. In the present case the momentum equation is adequately represented by

$$(\ell f'')' + ff'' = 0 \tag{68}$$

The external flow at the edge of the boundary layer is considered to be isoenergetic. This leads to $\frac{dI_e}{ds} = 0$ and the removal of the first term on the right-hand side of equation (66). The external flow at the boundary-layer edge is evaluated from equilibrium calculations. The species mass fractions are assumed to be frozen at these equilibrium values in the case of both the flat plate and stagnation point. This leads to the elimination of the first term on the right-hand side of equation (67). As discussed in the analysis section, this report considers the case in which no chemical reactions occur in the boundary layer and all reactions are at equilibrium in an infinitesimal layer at the wall. The rate of generation of the various chemical species in the boundary layer is then zero; hence $\dot{w}_i = 0$. Finally, with the assumption of Prandtl, Schmidt, and Lewis numbers equal to unity, equations (66) and (67) may be written

$$\left(\frac{\ell}{P} g'\right)' + fg' = 0 \tag{69}$$

$$\left(\frac{\ell}{S} Z_i'\right)' + fZ_i' = 0 \tag{70}$$

It is evident that equations (68) to (70) are of identical form and may be written

$$\left(\frac{\ell}{\phi} \lambda'\right)' + f\lambda' = 0 \tag{71}$$

where λ is f', g, or Z_i and ϕ is 1, P, or S. It is clear that f', g, and Z_i are linearly related when $P = S = 1$ since they all satisfy the same differential equation. The functions f' and g are also linearly proportional to the elemental mass fractions because the latter are proportional to Z_i. The boundary conditions associated with equation (71) are

$$\lambda(0) = \lambda_E, \quad \lambda'(0) = \lambda_E', \quad \lambda(\infty) \to 1$$

Equation (71) is readily integrated with ϕ and ℓ as constants to yield

$$\lambda' = \lambda'(0) \exp\left(-\int_0^{\eta} \frac{\phi}{\ell} f \, d\eta^{**}\right) \tag{72}$$

and

$$\lambda = \lambda(0) + \lambda'(0) \int_0^{\eta} \exp\left(-\int_0^{\eta^*} \frac{\phi}{\ell} f \, d\eta^{**}\right) d\eta^* \tag{73}$$

Let

$$G(\eta, \phi) = \int_0^{\eta} \frac{\phi}{\ell} \exp\left(-\int_0^{\eta^*} \frac{\phi}{\ell} f \, d\eta^{**}\right) d\eta^* \tag{74}$$

so that using equation (73) and the boundary conditions $\lambda'(0)$ and $\lambda(\eta)$,

$$\lambda'(0) = \frac{1 - \lambda(0)}{\frac{\ell}{\phi} G(\infty, \phi)} \tag{75}$$

and

$$\lambda(\eta) = \lambda(0) + [1 - \lambda(0)] \frac{G(\eta, \phi)}{G(\infty, \phi)} \tag{76}$$

It is evident from equation (75) that if $G(\infty, \phi)$ is known, $g'(0)$ and $Z_i'(0)$ and, therefore, the convective heat transfer can be determined, since

$$g'(0) = \frac{1 - g(0)}{\frac{\ell}{P} G(\infty, P)} \tag{77a}$$

and

$$Z_i'(0) = \frac{1 - Z_i(0)}{\frac{\ell}{S} G(\infty, S)} \tag{77b}$$

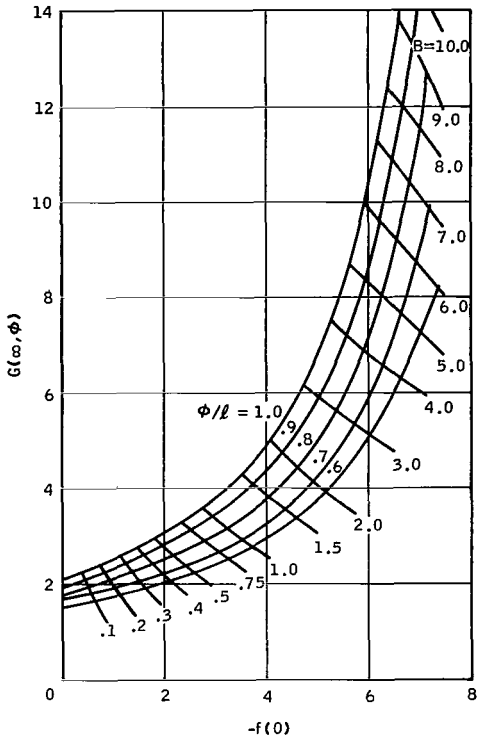

Figure 1. - Heat transfer parameter.

Constant property solutions of equation (71) are available in references 10 and 11. Results from these references are presented in figure 1 which relates $G(\infty, \phi)$ to $f(0)$. The mass injection parameter B may be related to these functions using

$$f(0) = \frac{B}{G(\infty, \phi)} \tag{78}$$

which follows from equations (22), (61), and (92).

Thus, given $P = S = 1$, ℓ, and B, the heat transfer parameters g' and Z' are readily obtained from figure 1 and equation (77).

Property Determination

Dorrance (ref. 5) recommends the use of the reference temperature in evaluating ℓ. The concept of a reference temperature has been utilized for some time in simulating the results of variable property solutions of the boundary-layer equations. Eckert (ref. 12) defines a reference temperature as follows

$$T^+ = 0.5T_e + 0.038T_e M_e{}^{*2} + 0.5T_E \tag{79}$$

The evaluation of ℓ using the reference temperature is straightforward for air or pure gases whose properties are well known. In the present case, however, the question arises as to the proper method of evaluating ℓ for a mixture of gases. The following approach is adopted:

(1) The viscosity is taken as the viscosity of air at the temperature T^+ using the Sutherland equation

$$\mu = 3.06 \times 10^{-8} \frac{T^{3/2}}{T + 112} \tag{80}$$

where T is in °K and μ in $\frac{\text{lb-sec}}{\text{ft}^2}$.

(2) The molecular weight $\overline{M}$ is calculated using the arithmetic mean of the species mass fractions at the wall and the boundary-layer edge as

$$\overline{M} = \left[\sum_i \left(\frac{C_{i,M}}{M_i} \right) \right]^{-1} \tag{81}$$

where

$$C_{i,M} = \frac{C_{i,e} + C_{i,E}}{2} \tag{82}$$

(3) The density may then be calculated from the perfect gas law

$$\rho(T^+) = \frac{p_e \overline{M}}{\mathcal{R} T^+} \tag{83}$$

This approximate approach for evaluating $\ell(T^+)$ was compared with a more detailed calculation for the stagnation-point boundary layer in which species mass fractions were obtained at the point in the frozen boundary layer where the temperature is T^+. These species mass fractions were then used to evaluate the molecular weight and viscosity. No significant difference was obtained between the results of this tedious calculation and the simple method presented herein. In view of existing uncertainties in parameters necessary for detailed calculations of transport properties at high temperatures and the approximate nature of the present analysis, it is thought that more sophisticated approaches are unwarranted.

Convective Heat Transfer

Heat transfer at the carbon surface is assumed to be the result of thermal conduction and the transport of chemical energy which is released or absorbed at the wall

because of chemical reaction. The wall heat flux is assumed proportional to the gradients of temperature and species mass fraction at the edge of the equilibrium layer

$$-\dot{q}_E = -\dot{q}_w = \left(K \frac{\partial T}{\partial y} + \rho D \sum_i h_i \frac{\partial C_i}{\partial y} \right)_E \tag{84}$$

The temperature gradient may be related to the enthalpy gradient by

$$\left(\frac{\partial I}{\partial y} \right)_E = \left(\sum_i \int_0^T c_{p,i} \, dT \frac{\partial C_i}{\partial y} + \sum_i C_i c_{p,i} \frac{\partial T}{\partial y} + \sum_i h_i^o \frac{\partial C_i}{\partial y} \right)_E \tag{85}$$

The frozen specific heat $c_{p,f}$ may now be introduced where

$$c_{p,f} = \sum_i C_i c_{p,i} \tag{86}$$

so that

$$\left(\frac{\partial T}{\partial y} \right)_E = \left[\frac{1}{c_{p,f}} \left(\frac{\partial I}{\partial y} - \sum_i h_i \frac{\partial C_i}{\partial y} \right) \right]_E \tag{87}$$

where

$$\sum_i \int_0^T c_{p,i} \, dT \frac{\partial C_i}{\partial y} + \sum_i h_i^o \frac{\partial C_i}{\partial y} = \sum_i \left(\int_0^T c_{p,i} \, dT + h_i^o \right) \frac{\partial C_i}{\partial y} = \sum_i h_i \frac{\partial C_i}{\partial y} \tag{88}$$

Thus equation (84) becomes

$$-\dot{q}_w = \left(\frac{k}{c_{p,f}} \right)_E \left[\frac{\partial I}{\partial y} + (L - 1) \sum_i h_i \frac{\partial C_i}{\partial y} \right]_E \tag{89}$$

It is seen that, when the Lewis number is unity, the heat-transfer rate is proportional to the enthalpy gradient at the edge of the equilibrium layer. Rather than setting the Lewis number equal to 1 at this point, the term explicitly displaying the gradient of the mass fraction is retained.

The heat-transfer equation may be transformed into the η coordinate using equations (57), (64), and (65)

$$-\dot{q}_w = \frac{\ell \rho_e \mu_e u_e r^\nu}{(2\bar{s})^{1/2} P} I_e \left[g_E' + (L - 1) \frac{\sum_i C_{i,e} h_{i,E} Z'_{i,E}}{I_e} \right] \tag{90}$$

where the Prandtl number $P = \frac{\mu_E c_{p,f,E}}{k_E}$ is also not set equal to unity at this point.

Using equation (77), g'_E and $Z'_{i,E}$ are eliminated yielding

$$-\dot{q}_w = \rho_e u_e C_H (I_e - I_E) \left[1 + \frac{G(\infty, P)}{G(\infty, S)} \left(\frac{L - 1}{L} \right) \frac{\sum_i h_{i,E} (C_{i,e} - C_{i,E})}{I_e - I_E} \right] \tag{91}$$

where

$$\rho_e u_e C_H = \frac{\rho_e \mu_e u_e r^\nu}{(2\bar{s})^{1/2} G(\infty, P)} \tag{92}$$

It is evident that, if the Lewis number is set equal to 1, the term in brackets in equation (91) becomes unity. For the case of $L = 1$, two implicit effects of mass injection on the heat flux are evident. First, mass injection causes an increase in $G(\infty, 1)$ and a resultant decrease in the Stanton number C_H. Secondly, variations in the enthalpy of the equilibrium layer, I_E, will be caused by species variations. It is seen also that, when $L > 1$, an additional term is obtained which increases the heat transfer due to increased diffusion of chemical potential energy.

Heat Balance on Fluid-Solid Interface

In order to determine the net heat transferred from the boundary layer to the surface, it is necessary to examine the various energy fluxes crossing the gas-solid

interface. The following sketch schematically indicates the components of the energy balance at the interface.

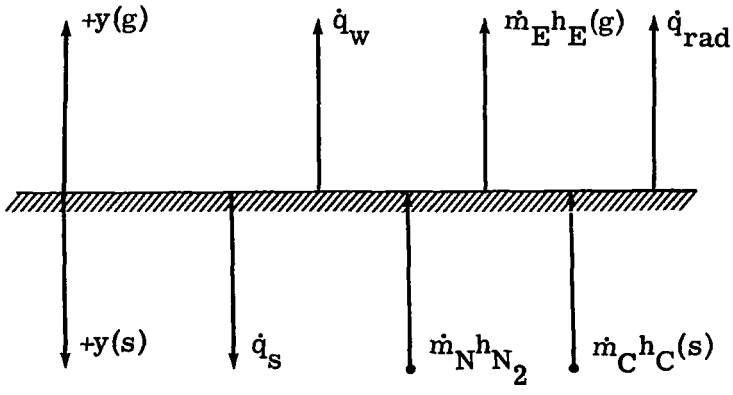

It is assumed that the gases flowing over the surface are nonradiating and transparent to the surface radiation $\dot{q}_{rad}$. The heat balance may be written

$$\dot{q}_s = -\dot{q}_w - \dot{q}_{rad} + \dot{m}_N h_{N_2,\,E} + \dot{m}_C h_{C,\,E}(s) - \dot{m}_E h_E(g) \tag{93}$$

The enthalpy of carbon in the solid phase is related to the enthalpy of carbon in the gaseous phase at the same temperature by the heat of sublimation of carbon as follows

$$h_C(s) + L_{vc} = h_C(g) \tag{94}$$

Therefore, combining equations (93) and (94), the heat flux to the surface becomes

$$\dot{q}_s = -\dot{q}_w - \dot{q}_{rad} + \dot{m}_N h_{N_2,\,E} + \dot{m}_C h_{C,\,E}(g) - \dot{m}_C L_{vc} - \dot{m}_E h_E(g) \tag{95}$$

The mass flux $\dot{m}_E$ can be eliminated from equation (95) by using equation (10) to obtain

$$\dot{q}_s = -\dot{q}_w - \dot{q}_{rad} + \dot{m}_N h_{N_2,\,E} + \dot{m}_C h_{C,\,E}(g) - \dot{m}_C L_{vc} - \left(\dot{m}_N + \dot{m}_C\right) h_E(g) \tag{96}$$

Finally, by using equation (91), the surface heat flux can be expressed as

$$\dot{q}_s = \rho_e u_e C_H \left[I_e - I_E + \frac{G(\infty, P)}{G(\infty, S)} \left(\frac{L - 1}{L} \right) \sum_i h_{i,E} \left(C_{i,e} - C_{i,E} \right) - \frac{\dot{q}_{rad}}{\rho_e u_e C_H} \right.$$

$$\left. + \frac{\dot{m}_N}{\rho_e u_e C_H} \left(h_{N_2,E} - h_E(g) \right) + \frac{\dot{m}_C}{\rho_e u_e C_H} \left(h_{C,E}(g) - h_E(g) \right) - \frac{\dot{m}_C}{\rho_e u_e C_H} L_{vc} \right] \tag{97}$$

It is seen from the enthalpy terms that the injection of nitrogen, in addition to those effects discussed previously, modifies the net energy flux to the surface.

Stagnation-Point Problem

Up to this point the analysis has been applicable to flat plate and stagnation-point boundary-layer problems, and to other configurations in the context of local similarity and negligible pressure gradient. Inasmuch as the stagnation-point problem is of greatest interest in current technology, this case is developed in more detail here.

The velocity in the vicinity of a stagnation point is of the form

$$u_e = \left(\frac{du_e}{dS} \right)_{sp} S \tag{98}$$

where $\left(\frac{du_e}{dS} \right)_{sp}$ is evaluated using the familiar Newtonian velocity gradient formula

$$\left(\frac{du_e}{dS} \right)_{sp} = \frac{1}{R} \left(2 \frac{p_e - p_\infty}{\rho_e} \right)^{1/2} \tag{99}$$

From equation (58), $\bar{s}$ can be evaluated as

$$\bar{s} = \int_0^S \rho_e \mu_e r^{2\nu} u_e \, dS = \rho_e \mu_e \left(\frac{du_e}{dS} \right)_{sp} \frac{S^{2(\nu+1)}}{2(\nu + 1)} \tag{100}$$

Equation (92) then yields

$$\rho_e u_e C_H = \rho_e \mu_e{}^{1/2} \left(\frac{du_e}{dS}\right)_{sp}^{1/2} \frac{(\nu + 1)^{1/2}}{G(\infty, P)} \tag{101}$$

The mass fluxes of nitrogen and carbon across the gas-solid interface are then

$$\dot{m}_N = \left(\frac{\dot{m}_N}{\rho_e u_e C_H}\right) \left(\rho_e \mu_e\right)^{1/2} \left(\frac{du_e}{dS}\right)_{sp} \frac{(\nu + 1)^{1/2}}{G(\infty, P)} \tag{102}$$

$$\dot{m}_C = \left(B - \frac{\dot{m}_N}{\rho_e u_e C_H}\right) \left(\rho_e \mu_e\right)^{1/2} \left(\frac{du_e}{dS}\right)_{sp}^{1/2} \frac{(\nu + 1)^{1/2}}{G(\infty, P)} \tag{103}$$

The convective and diffusive heat fluxes at the wall for Lewis and Prandtl numbers of 1 are given by

$$-\dot{q}_w = \left(\rho_e \mu_e\right)^{1/2} \left(\frac{du_e}{dS}\right)^{1/2} \frac{(\nu + 1)^{1/2}}{G(\infty, 1)} \left(I_e - I_E\right) \tag{104}$$

and the heat flux penetrating the surface of the material is

$$\dot{q}_S = \left(\rho_e \mu_e\right)^{1/2} \left(\frac{du_e}{dS}\right)_{sp}^{1/2} \frac{(\nu + 1)^{1/2}}{G(\infty, 1)} \left[I_e - I_E + \left(\frac{\dot{m}_N}{\rho_e u_e C_H}\right) h_{N_2, E} + \left(B - \frac{\dot{m}_N}{\rho_e u_e C_H}\right) h_{C, E}(g) - \left(B - \frac{\dot{m}_N}{\rho_e u_e C_H}\right) L_{vc} - B h_E(g) - \frac{\dot{q}_{rad}}{\rho_e u_e C_H}\right] \tag{105}$$

The mass flux of carbon across the interface is proportional to the rate of surface recession since

$$\dot{m}_C = \rho_C \frac{d\tau}{dt} \tag{106}$$

where τ is the thickness of the carbon material at the stagnation point. The surface ablation rate is then determined from

$$\frac{d\tau}{dt} = \frac{1}{\rho_C}\left(B - \frac{\dot{m}_N}{\rho_e u_e C_H}\right)\left(\rho_e \mu_e\right)^{1/2}\left(\frac{du_e}{dS}\right)^{1/2}\frac{(\nu+1)^{1/2}}{G(\infty, 1)} \tag{107}$$

The thickness of carbon ablated during an arbitrary heating period is given by integration of equation (107)

$$\tau = \int_0^t \frac{B - \dfrac{\dot{m}_N}{\rho_e u_e C_H}}{\rho_C}\left(\rho_e \mu_e\right)^{1/2}\left(\frac{du_e}{dS}\right)_{sp}^{1/2}\frac{(\nu+1)^{1/2}}{G(\infty, 1)}\,dt \tag{108}$$

RESULTS AND DISCUSSION

Calculations have been performed to demonstrate the accuracy of the approximation of the present work in comparison with existing results for the case of no nitrogen injection and to evaluate the effects of nitrogen injection. All calculations pertain to the stagnation-point boundary layer. The method of determination of boundary-layer-edge properties and composition has been outlined. Properties and species mass fractions, so obtained, are tabulated in table I. It is seen that at these flight conditions oxygen is completely dissociated and significant nitrogen dissociation has occurred.

TABLE I. - FREE-STREAM AND STAGNATION-POINT CONDITIONS

[Velocity = 19 700 ft/sec]

Case	Altitude, kft	I_e, Btu/lb	p_e, atm	T_e, °K	M_e/M_a	ρ_e, lb/ft^3	$C_{N,e}$	$C_{N_2,e}$	$C_{O,e}$	$C_{O_2,e}$
a	115	7864	2.985	6750	1.379	7.070×10^{-3}	0.19	0.58	0.23	$<10^{-3}$
b	150	7875	.605	6220	1.402	1.530	.21	.56	.23	$<10^{-3}$
c	180	7877	.2026	5900	1.418	.535	.21	.56	.23	$<10^{-3}$
d	200	7872	.0966	5750	1.425	.260	.24	.53	.23	$<10^{-3}$
e	220	7862	.0458	5560	1.431	.126	.25	.52	.23	$<10^{-3}$

Table II presents calculations of enthalpy, mass injection parameters, and species mass fractions in the equilibrium layer for a wall temperature of 2000° K. Equilibrium constants for equations (2) to (4) and species properties in the equilibrium layer were obtained from reference 13. In the diffusion-controlled regime it is found that only molecular nitrogen and carbon monoxide exist in significant amounts in the equilibrium layer. This is in agreement with the findings of reference 3 for no nitrogen injection. At 2000° K, for instance, the ratios of the partial pressure of other species to the total pressure were found to be on the order of 10^{-10} or less. It was also found from equation (43) that the relative proportions of nitrogen and carbon monoxide in the equilibrium layer depend only on the nitrogen injection parameter $\frac{\dot{m}_N}{\rho_e u_e C_H}$. Increasing values of $\frac{\dot{m}_N}{\rho_e u_e C_H}$, of course, reduce the mass fraction of carbon monoxide at the wall.

TABLE II. - EQUILIBRIUM LAYER PROPERTIES

$\left[T_w = 2000° \text{ K}\right]$

$\frac{\dot{m}_N}{\rho_e u_e C_H}$	$C_{CO, E}$	$C_{N_2, E}$	$\frac{\dot{m}_C}{\rho_e u_e C_H}$	B	$I_{E'}$ Btu/lb
0	0.344	0.656	0.173	0.173	284
.5	.242	.758	.173	.673	455
1.0	.186	.814	.173	1.173	548
2.0	.128	.872	.173	2.173	646
3.0	.097	.903	.173	3.173	698
4.0	.078	.922	.173	4.173	731
6.0	.056	.944	.173	6.173	769

It can be demonstrated that the carbon mass flux parameter $\frac{\dot{m}_C}{\rho_e u_e C_H}$ is independent of the nitrogen mass injection parameter as shown in table II. Elimination of

B + 1 in equation (23) using equation (25) allows expression of the carbon mass flux parameter in terms of boundary-layer-edge oxygen mass fraction only

$$\frac{\dot{m}_C}{\rho_e u_e C_H} = \frac{3}{4} \bar{C}_{O,e} \tag{109}$$

While $\frac{\dot{m}_C}{\rho_e u_e C_H}$ is invariant with increases in the nitrogen injection parameter, it is evident that the carbon mass loss is reduced due to the decreased Stanton number resulting from the increased total mass injection. The reduction in carbon mass loss with increasing $\frac{\dot{m}_N}{\rho_e u_e C_H}$ and increasing altitude is demonstrated in figure 2. Increasing the altitude reduces the carbon mass loss due to the decreasing flux of oxygen available from the free stream for reaction.

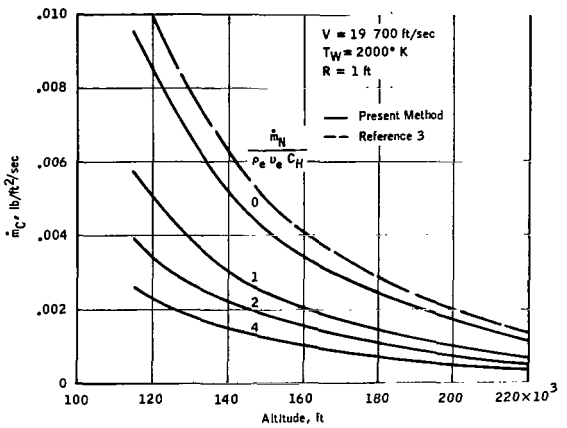

Figure 2. - Effects of nitrogen injection and altitude on carbon mass loss.

As discussed previously, perhaps the most accurate and sophisticated analysis for the ablation of graphite appears in reference 3. For the special case of $\frac{\dot{m}_N}{\rho_e u_e C_H} = 0$, the results of the present analysis are compared with the carbon mass loss obtained from reference 3. It is seen that the present results are consistently lower by about 10 to 15 percent. Differences of this magnitude are not surprising in view of the vast differences between the present model and that of reference 3.

The variation of total mass flux from the equilibrium layer is shown in figure 3 as a function of the nitrogen injection parameter. It is seen that the total mass flux increases rapidly for small values of the injection parameter. At larger values of $\frac{\dot{m}_N}{\rho_e u_e C_H}$, the increase is less marked. This behavior results from the fact that C_H

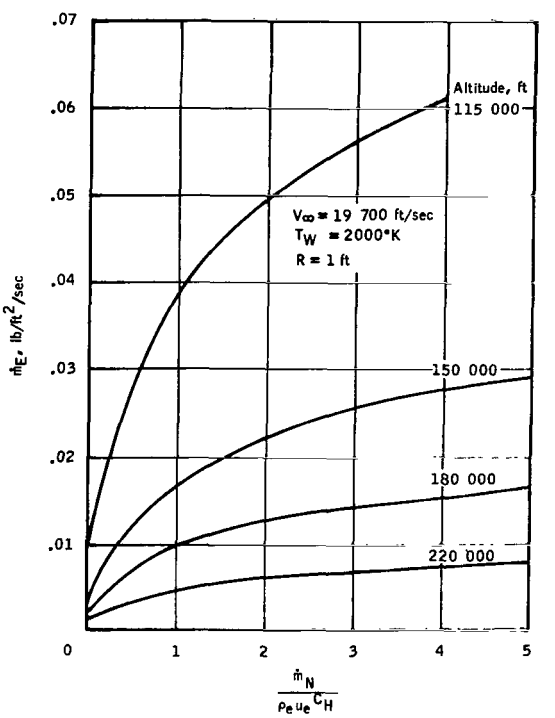

Figure 3. - Total mass loss rate.

decreases rapidly for large values of mass injection, resulting in small increases in total mass flux as $\frac{\dot{m}_N}{\rho_e u_e C_H}$ is increased.

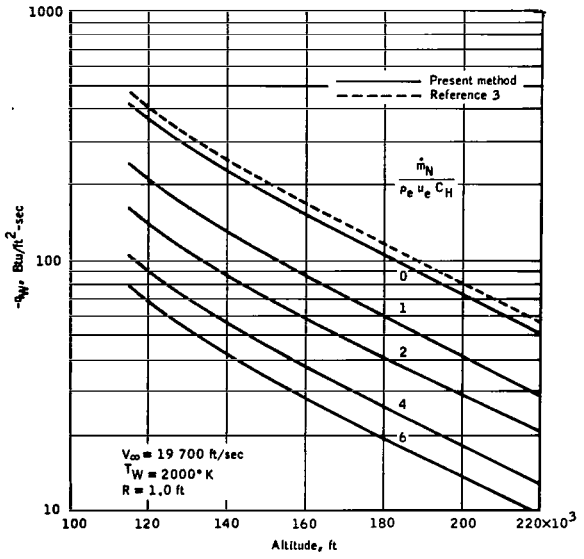

Figure 4. - Aerodynamic heating rate.

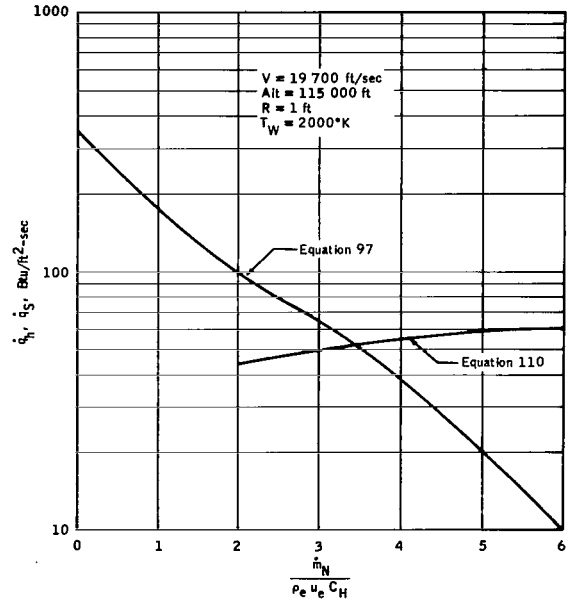

Figure 5. - Surface heat flux absorbed.

A comparison of the aerodynamic heat flux with carbon ablation from the present analysis and reference 3 is shown in figure 4. Differences of about 10 percent are evident. In view of the close correspondence of the present results to those of the sophisticated work of reference 3, it is felt that considerable confidence may be placed in the present analysis. It is also evident from figure 4 that nitrogen injection provides substantial reductions in heat flux. This is attributable primarily to large reductions in the Stanton number due to blowing.

The heat flux absorbed by the graphite surface as calculated by equation (97) is shown in figure 5 as a function of the injection parameter for an altitude of 115 000 feet. It is seen that nitrogen injection strongly reduces the heat flux absorbed.

The results presented have all assumed that an unidentified mechanism controlled the surface temperature at a fixed value. Usually, at a given flight condition, the wall temperature will be determined by the rate of radiation cooling, mass loss, and internal conduction. It is of interest to estimate the nitrogen injection required to maintain the wall at a specified wall temperature. In the case of steady ablation the surface temperature is determined by a balance of the net heat flux crossing the solid-gas interface and of the enthalpy transport of carbon and nitrogen from the initial temperature T_{in}

$$\dot{q}_h = \dot{m}_C \int_{T_{in}}^{T_w} c_{p,C}(s)\, dT + \dot{m}_N \int_{T_{in}}^{T_w} c_{p,N_2}\, dT \qquad (110)$$

This expression is plotted in figure 5 for $T_{in} = 300^\circ$ K and $T_w = 2000^\circ$ K. The intersection of the two curves shows that a wall temperature of 2000° K is obtained at the listed flight conditions with a nitrogen mass injection parameter $\frac{\dot{m}_N}{\rho_e u_e C_H} = 3.5$. Figures 2 and 3 show that this corresponds to graphite and nitrogen expenditures of 0.0029 and 0.056 lb/ft^2-sec, respectively.

A widely used parameter in evaluating the merit of a heat-protection system is the effective heat of ablation. It is a measure of the thermal energy accommodated per unit mass loss of the heat-protection system. The effective heat of ablation as conventionally defined is

$$h_{eff} = \frac{\left(-\dot{q}_w\right)_{N.B.}}{\dot{m}_C} \tag{111}$$

where $\left(-\dot{q}_w\right)_{N.B.}$ is the aerodynamic heat transfer without mass injection. Using equations (103) and (104) with $I_E = I_A$, the effective heat of ablation becomes

$$h_{eff} = \frac{\left(I_e - I_A\right)}{\left(B - \frac{\dot{m}_N}{\rho_e u_e C_H}\right)} \frac{\left(C_H\right)_{N.B.}}{C_H} \tag{112}$$

The effective heat of ablation is plotted in figure 6 as a function of the enthalpy difference $I_e - I_A$, where I_A is the enthalpy of air at wall temperature and pressure. Again comparison with the results of reference 3 shows satisfactory agreement for the case of no nitrogen injection. It is seen that, as judged by h_{eff}, substantial gains are made in ablation efficiency as a result of mass injection. This result demonstrates that, if mass loss of graphite is critical, nitrogen injection may be employed to reduce surface ablation substantially. Clearly, other parameters, which show less favorable comparisons, may be defined to represent the ablation efficiency. Care

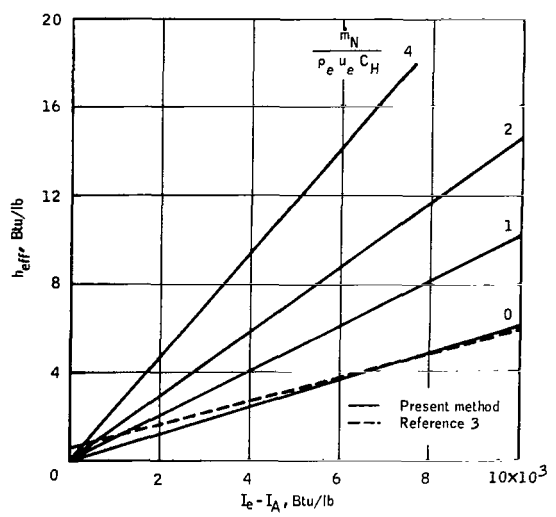

Figure 6. - Effective heat of ablation.

should be taken, therefore, in judging heat-protection-system efficiency based on parameters such as h_{eff}.

CONCLUDING REMARKS

The effects of nitrogen injection on the heat and mass transfer of an ablating surface have been analyzed based on a model which considers all chemical reactions to occur in an infinitesimal region adjacent to the surface. Diffusion of oxygen through a frozen boundary layer and chemical equilibrium in the equilibrium layer have been assumed to control the rate of mass loss of carbon. Equations have been derived for the species mass fractions and mass injection parameters as well as for the heat and mass transfer rates. It has been demonstrated that:

(1) The carbon mass injection parameter is independent of nitrogen injection in the diffusion-controlled regime and, in fact, depends only on the mass fraction of oxygen at the boundary-layer edge.

(2) The only species present at the wall in significant quantities are nitrogen and carbon monoxide. Injection of nitrogen increases the wall mass fraction of nitrogen at the expense of the carbon monoxide mass fraction.

(3) The injection of nitrogen affects heat transfer by reducing the heat transfer coefficient as a result of increased blowing into the boundary layer and through modifications of the enthalpy of gases at the wall.

(4) When minimization of carbon surface recession is important, injection of nitrogen can substantially reduce the carbon mass loss.

Manned Spacecraft Center
National Aeronautics and Space Administration
Houston, Texas, March 23, 1967
914-50-10-01-72

REFERENCES

1. Dennison, M. R.; and Dooley, D. A.: Combustion in the Laminar Boundary Layer of Chemically Active Sublimating Surfaces. J. Aeron. Sci., Apr. 1958.

2. Scala, Sinclaire M.: The Ablation of Graphite in Dissociated Air. Gen. Elec. Sp. Sci. Lab. Rept. R 62 SD 72.

3. Scala, S. M.; and Gilbert, L. M.: The Sublimation of Graphite at Hypersonic Speed. AIAA Entry Technology Conference, Williamsburg, Va., Oct. 12-14, 1964.

4. Lees, Lester: Convective Heat Transfer with Mass Addition and Chemical Reactions. Third AGARD Colloquium on Combustion and Propulsion, Palermo, Sicily, Pergamon Press, 1959.

5. Dorrance, William H.: Viscous Hypersonic Flow. McGraw-Hill Book Company, 1962.

6. Fay, J. A.; and Riddell, F. R.: Theory of Stagnation Point Heat Transfer in Dissociated Air. J. Aeron. Sci., vol. 25, 1958, pp. 73-85.

7. Moeckel, W. E.; and Weston, Kenneth C.: Composition and Thermodynamic Properties of Air in Chemical Equilibrium. NACA TN 4265, Apr. 1958.

8. Thorn, R. J.; and Winslow, G. H.: Vaporization Coefficient of Graphite and Composition of the Equilibrium Vapor. J. Chem. Phys., vol. 26, Jan. 1957.

9. Lees, Lester: Laminar Heat Transfer over Blunt Nosed Bodies at Hypersonic Flight Speeds. Jet Propulsion, vol. 26, 1956, pp. 259-269.

10. Mickley, H. S.; Ross, R. C.; Squyers, A. L.; and Stewart, W. E.: Heat, Mass, and Momentum Transfer for Flow Over a Flat Plate with Blowing or Suction. NACA TN 3208, July 1954.

11. Emmons, H. W.; and Leigh, D.: Tabulation of the Blasius Function with Blowing and Suction. Harvard University Division of Applied Sciences, Combustion Aerodynamics Laboratory Interim Technical Report No. 9, Nov. 1953.

12. Eckert, E. R. G.: Engineering Relations for Friction and Heat Transfer to Surfaces in High Velocity Flow. J. Aeron. Sci., vol. 22, Aug. 1955, pp. 585-587.

13. McBride, Bonnie J.; Heimel, Sheldon; Ehlers, Janet G.; and Gordon, Sanford: Thermodynamic Properties to 6000° K for 210 Substances Involving the First 18 Elements. NASA SP-3001, 1963.

"The aeronautical and space activities of the United States shall be conducted so as to contribute . . . to the expansion of human knowledge of phenomena in the atmosphere and space. The Administration shall provide for the widest practicable and appropriate dissemination of information concerning its activities and the results thereof."

—NATIONAL AERONAUTICS AND SPACE ACT OF 1958

NASA SCIENTIFIC AND TECHNICAL PUBLICATIONS

TECHNICAL REPORTS: Scientific and technical information considered important, complete, and a lasting contribution to existing knowledge.

TECHNICAL NOTES: Information less broad in scope but nevertheless of importance as a contribution to existing knowledge.

TECHNICAL MEMORANDUMS: Information receiving limited distribution because of preliminary data, security classification, or other reasons.

CONTRACTOR REPORTS: Scientific and technical information generated under a NASA contract or grant and considered an important contribution to existing knowledge.

TECHNICAL TRANSLATIONS: Information published in a foreign language considered to merit NASA distribution in English.

SPECIAL PUBLICATIONS: Information derived from or of value to NASA activities. Publications include conference proceedings, monographs, data compilations, handbooks, sourcebooks, and special bibliographies.

TECHNOLOGY UTILIZATION PUBLICATIONS: Information on technology used by NASA that may be of particular interest in commercial and other non-aerospace applications. Publications include Tech Briefs, Technology Utilization Reports and Notes, and Technology Surveys.

Details on the availability of these publications may be obtained from:

SCIENTIFIC AND TECHNICAL INFORMATION DIVISION

NATIONAL AERONAUTICS AND SPACE ADMINISTRATION

Washington, D.C. 20546